EuroIntervention 2014;10:303-311 published online ahead of print April 2014

Combined NIRS and IVUS imaging detects vulnerable plaque using a single catheter system: a head-to-head comparison with OCT

Tomasz Roleder[1], MD, PhD; Jason C. Kovacic[1], MD, PhD; Ziad Ali[2], MD, PhD; Raman Sharma[1]; Ecatarina Cristea[1], MD ; Pedro Moreno[1], MD; Samin K. Sharma[1], MD; Jagat Narula[1], MD, PhD; Annapoorna S. Kini[1]*, MD

1. Mount Sinai Medical Center and Mount Sinai School of Medicine, New York, NY, USA; 2. Cardiovascular Research Foundation, New York, NY, USA

This paper also includes accompanying supplementary data published online at: http://www.pcronline.com/eurointervention/74th_issue/53

KEYWORDS

- intravascular ultrasound
- near-infrared spectroscopy
- optical coherence tomography
- vulnerable plaque

Abstract

Aims: The presence of thin-cap fibroatheromas (TCFA) is associated with high risk of acute coronary syndrome, hence their early detection may identify high-risk patients. In the present study we investigated the ability of a combined imaging catheter with near-infrared spectroscopy (NIRS) plus intravascular ultrasound (IVUS) to detect TCFA in patients with stable coronary artery disease.

Methods and results: Optical coherence tomography (OCT) and combined NIRS-IVUS assessment were performed on identical coronary segments. IVUS analysis provided per-segment minimal cross-sectional area (CSA), plaque length (PL), plaque burden (PB), plaque volume (PV), and remodelling index (RI). OCT was used as the gold-standard reference to define TCFA (fibrous cap thickness <65 µm). Plaque lipid content was estimated by NIRS (lipid core burden index [LCBI]). OCT-defined TCFA was present in 18 of 76 segments. IVUS revealed that OCT-defined TCFA were positively remodelled lesions with greater PB and PV, smaller CSA, and longer PL, while NIRS revealed greater LCBI per 2 mm segment ($LCBI_{2\,mm}$) (all $p<0.001$). Greatest accuracy for OCT-defined TCFA detection was achieved using $LCBI_{2\,mm}$ >315 with RI >1.046 as a combined criterion value.

Conclusions: OCT-defined TCFA are characterised by positive vessel remodelling, high plaque burden and greater lipid core burden as assessed by dual NIRS-IVUS imaging.

**Corresponding author: Mount Sinai Medical Center and Mount Sinai School of Medicine, One Gustave L. Levy Place, Box 1030, New York, NY, 10029, USA. E-mail: annapoorna.kini@mountsinai.org*

SUBMITTED ON 08/07/2013 - REVISION RECEIVED ON 10/09/2013 - ACCEPTED ON 30/09/2013

DOI: 10.4244/EIJV10I3A53

Introduction

Atherosclerotic coronary artery plaque rupture leads to intravascular thrombus formation, which may culminate in an acute coronary event with myocardial ischaemia. Rupture-prone atherosclerotic plaques are known as "vulnerable plaques". They are characterised by outward vessel expansion (positive remodelling), a high burden of intra-plaque lipid, macrophage infiltration and a thin fibrous cap (<65 µm)[1-3]. Histopathologically, these plaques are referred to as "thin-cap fibroatheromas" (TCFA). The presence of TCFA is associated with increased risk of acute coronary syndrome[4], hence their early detection may help to stratify high-risk patients.

Optical coherence tomography (OCT) is the principal imaging tool used to detect TCFA. The high imaging resolution of OCT (10-20 µm) permits the measurement of fibrous cap thickness and also the classification of plaques as being fibrous, calcified or lipid-rich[5]. However, OCT is limited by its low depth penetration into the vessel wall (2 mm), which hampers accurate assessment of necrotic core depth and vessel remodelling[6-8]. Moreover, OCT imaging requires the evacuation or replacement of blood from the vessel, and it is poorly suited to assessing aorto-ostial coronary lesions. As an alternative modality, greyscale intravascular ultrasound (IVUS) imaging does not require the evacuation of blood and has superior depth penetration with a unique ability to measure plaque burden and vessel remodelling[9]. However, due to substantially inferior resolution (100-150 µm), IVUS is unable to measure cap thickness to the required accuracy to diagnose TCFA directly[10], and it does not provide distinction between lipid-rich and non-lipid-rich plaques[11].

The recent combination of near-infrared spectroscopy (NIRS) with greyscale IVUS in a single imaging catheter allows simultaneous assessment of plaque composition both in terms of its chemical (by NIRS) and morphologic (by IVUS) characteristics. Specifically, NIRS provides the ability to quantify plaque lipid content[12,13]. The validity of this dual modality catheter was provided by prior studies in the setting of acute coronary syndrome, which documented that, while NIRS detects plaque composition[14], greyscale IVUS describes morphology[15]. A previous autopsy study demonstrated that NIRS is able to detect features associated with plaque vulnerability in humans[14]. In the present study, we investigated the ability of combined NIRS-IVUS imaging to detect OCT-defined TCFA in patients with stable coronary disease.

Editorial, see page 296

Methods

STUDY POPULATION

The current study employed intravascular OCT and combined NIRS-IVUS assessment of identical segments of the same patients' coronary arteries/plaques. All imaging was performed during the same procedure. The study group was selected from patients referred for cardiac catheterisation due to chronic stable coronary disease symptoms. Patients with renal failure (creatinine >1.5 mg/dl), haemodynamic compromise, contrast allergy, and aorto-ostial coronary artery lesions were excluded from the study. The segment to scan was selected at the operator's discretion after the diagnostic angiogram. One segment of coronary artery was defined as the region between two significant side branches. Analysed segments were both target and non-target regions in the imaged artery by OCT and NIRS-IVUS. None of the patients developed any complications due to OCT and combined NIRS-IVUS imaging, which were performed using bivalirudin anticoagulation (activated clotting time >300 sec) and following intracoronary nitroglycerine (100-200 µm) administration.

NIRS, IVUS and OCT images were analysed off-line together with angiographic quantitative coronary analysis (QCA). Coronary segments with incomplete and/or poor quality NIRS, IVUS or OCT scans were removed from the investigation (16 coronary segments), hence the ultimate analysis included 76 coronary segments assessed in 60 patients.

All patients were drawn from the Institutional Review Board (IRB) approved Clinical Interventional and Multimodality Imaging Database of The Mount Sinai Medical Center in New York, USA, and in accordance with the Code of Federal Regulations and the Declaration of Helsinki. All patients signed an informed consent before the procedure. All patients undergoing PCI are entered into this database within 24 hours of the index intervention. Details of the Clinical Interventional database have been published previously[15,16].

QUANTITATIVE CORONARY ARTERIOGRAPHY MEASUREMENTS

QCA was performed off-line using a validated cardiovascular measurement system (CMS) (QAngioXA software 7.3; Medis, Leiden, The Netherlands) for calculation of minimum lumen diameter, reference lumen diameter and % diameter stenosis with complete coronary segment morphology characteristics.

OPTICAL COHERENCE TOMOGRAPHY IMAGE ACQUISITION

The commercially available intravascular imaging system OCT C7 Dragonfly™ (St. Jude Medical, St. Paul, MN, USA) was used for OCT image acquisition. OCT image analysis scrutinised serial cross-sectional images for plaque composition, cross-sectional area (CSA), and vessel diameter. Plaque composition was analysed according to previously validated criteria for OCT **(Online Appendix)**[5,17]. OCT-defined TCFA was defined as a lipid-rich plaque with fibrous cap thickness <65 µm.

COMBINED NIRS AND GREYSCALE IVUS IMAGE ACQUISITION AND ANALYSIS

Combined NIRS and greyscale IVUS image acquisition was performed using the commercially available TVC Imaging System™ with the 2.4 Fr Insight™ Catheter (Infraredx, Inc., Burlington, MA, USA). The NIRS analysis allows calculation of lipid core burden index (LCBI) **(Online Appendix)**, and in the present study the maximal LCBI was estimated in 2 mm, 4 mm and 8 mm pullback compartments for every analysed lesion ($LCBI_{2\ mm}$, $LCBI_{4\ mm}$, $LCBI_{8\ mm}$, **Figure 1**).

Quantitative greyscale IVUS measurements were performed using QIvus version 2.1 (Medis, Leiden, The Netherlands) to quantify lumen CSA, external elastic lamina (EEM) CSA, plaque and media CSA, plaque burden, lumen and vessel volume and EEM

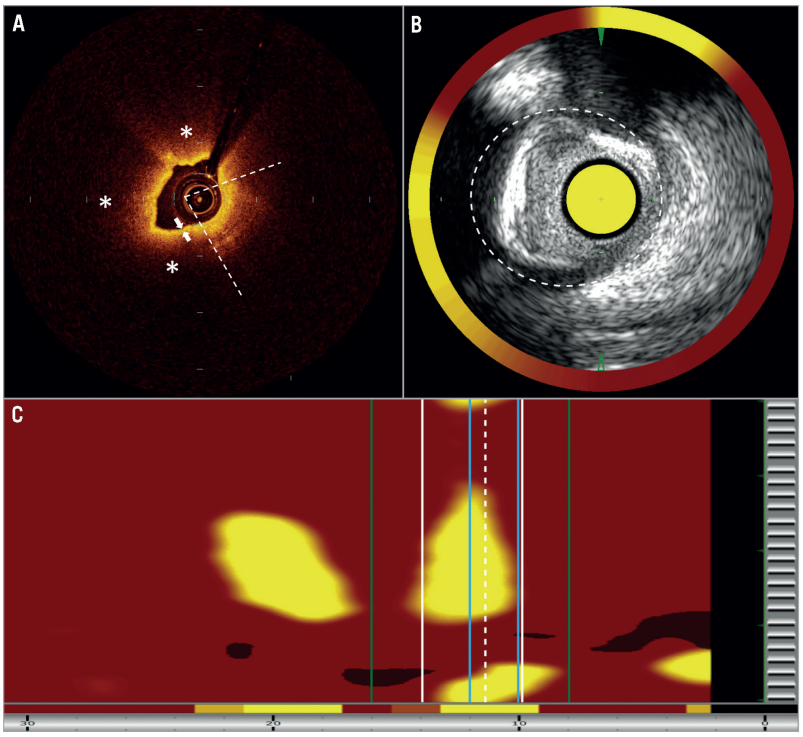

Figure 1. *Representative case of OCT-defined TCFA for greyscale IVUS and near-infrared spectroscopy. A) Optical coherence tomography showed lipid-rich plaque (*) with lipid arc=330° (open angle between two white dashed lines) and fibrous cap thickness 50 µm (white arrows). B) Greyscale IVUS showed minimal cross-sectional area (CSA)=1.95 mm², external elastic lamina (EEM) CSA=11.00 mm² (white dashed line); estimated plaque burden was 82.27% and the vessel was positively remodelled (reference EEM CSA was 9.53 mm²). C) NIRS revealed the maximum $LCBI_{2\ mm}$=592 (2 mm segment between the blue lines), maximum $LCBI_{4\ mm}$=416 (4 mm segment between white lines) and maximum $LCBI_{8\ mm}$=279 (8 mm segment between green lines).*

volume, and remodelling index (RI). Lesions with RI ≤0.95 were defined as negatively remodelled, while those with an RI ≥1.05 were defined as positively remodelled **(Online Appendix)**.

CO-REGISTRATION OF NIRS, GREYSCALE IVUS AND OCT

During the combined NIRS-IVUS pullback, anatomical landmarks were imprinted on the chemogram and bookmarked on the IVUS images, i.e., fiducial points, minimal vessel CSA and side branches. Those landmarks allowed matching of OCT images to corresponding sections of NIRS map, IVUS images and the coronary angiogram. Such co-registration allowed simultaneous judgement of LCBI values, IVUS measurements and OCT analysis in the same lesion of the coronary vessel.

The statistical analysis was performed using MedCalc software version 12.2.1 (MedCalc, Ostend, Belgium) **(Online Appendix)**.

Results

Sixty patients were enrolled into the study. Using OCT, we identified the presence of TCFA in 18 of 76 segments. There were no significant differences in clinical patient characteristics, pharmacological therapy and laboratory results between patients with and without TCFA **(Table 1)**. Angiographic QCA analysis is summarised in **Online Table 1**. Coronary segments with OCT-defined TCFA were characterised by higher % diameter stenosis and tended to have smaller minimal lumen diameter assessed by QCA. There were no differences between the groups in terms of lesion location and type.

IVUS analysis revealed that lesions with OCT-defined TCFA were positively remodelled and had greater plaque burden, greater plaque volume, smaller minimal CSA, and longer length **(Figure 2)**.

Plaque composition analysis showed that a wider lipid arc and higher maximal LCBI values in each of the 2 mm, 4 mm and 8 mm segment compartments characterised lesions with OCT-defined TCFA. Subclinical plaque rupture, as assessed by OCT, occurred only in OCT-defined TCFA. Data from greyscale IVUS, NIRS and OCT imaging are presented in **Table 2**.

NIRS DATA AND OCT-DEFINED PLAQUE CHARACTERISTICS

Maximal LCBI values correlated positively with OCT-defined maximal lipid arc (r=0.678 for $LCBI_{2\ mm}$, r=0.641 for $LCBI_{4\ mm}$, r=0.650 for $LCBI_{8\ mm}$; all p<0.001) and negatively with OCT-defined minimal fibrous cap thickness (r=–0.478 for $LCBI_{2\ mm}$, r=–0.450 for $LCBI_{4\ mm}$, r=–0.489 for $LCBI_{8\ mm}$; all p<0.001) **(Figure 2)**.

DIAGNOSTIC VALUE OF NIRS AND IVUS TO CLASSIFY OCT-DEFINED TCFA

Multivariable logistic regression analysis revealed that $LCBI_{2\ mm}$, $LCBI_{4\ mm}$, $LCBI_{8\ mm}$ and RI were independent predictors of OCT-defined TCFA **(Table 3, Online Table 2, Online Table 3)**. Receiver

Table 1. Clinical patient characteristics.

	Patients without TCFA (n=44)	Patients with TCFA (n=16)	*p*-value
Age (years), SD	62±11	59±10	0.430
Male gender, n (%)	33 (75)	15 (94)	0.092
Body mass index, kg/m^2 (IQR)	29 (26-32)	27 (24-30)	0.234
CCS III/IV, n (%)	26 (61)	7 (41)	0.176
Risk factors			
Hypertension, n (%)	43 (98)	14 (88)	0.124
Hyperlipidaemia, n (%)	41 (93)	16 (100)	0.895
Diabetes mellitus, n (%)	19 (43)	7 (44)	0.887
Current smoking, n (%)	6 (14)	3 (19)	0.692
Prior MI, n (%)	9 (20)	2 (12)	0.429
Number of diseased vessels			
1	17 (39)	9 (56)	
2	15 (34)	4 (25)	
3	12 (27)	3 (19)	0.579
SYNTAX score, (IQR)	9 (5-15)	9 (3-15)	0.898
Pharmacological therapy			
Aspirin, n (%)	41 (93)	14 (87)	0.528
Thienopyridine, n (%)	19 (44)	4 (25)	0.371
Beta-adrenergic antagonist, n (%)	33 (75)	11 (69)	0.725
Calcium-channel antagonist, n (%)	23 (52)	9 (56)	0.963
ARB/ACEI, n (%)	27 (61)	11 (69)	0.809
Statin, n (%)	33 (75)	13 (81)	0.434
Other lipid-lowering therapy, n (%)	4 (9)	1 (6)	0.682
Oral antidiabetics, n (%)	11 (25)	6 (38)	0.421
Insulin, n (%)	1 (2)	1 (6)	0.478
Laboratory results			
Troponin I	0.0	0.0	
White blood cell count (109/L), SD	7.26±2.49	7.47±1.66	0.754
Total cholesterol, mg/dl (IQR)	139 (120-171)	150 (133-186)	0.504
LDL cholesterol, mg/dl (IQR)	72 (65-111)	80 (66-103)	0.872
HDL cholesterol, mg/dl (IQR)	36 (33-43)	40 (33-45)	0.750
Triglyceride, mg/dl (IQR)	120 (82-147)	141 (111-177)	0.088
Haemoglobin A1c, %	6.5 (6.1-7.5)	8.4 (6.0-9.6)	0.355
hsCRP, mg/dl (IQR)	1.9 (0.9-4.9)	1.4 (0.6-2.5)	0.127
GRF (mL/min/1.73 m^2), SD	69±19	71±20	0.782

ACEI: angiotensin-converting enzyme inhibitor; ARB: angiotensin II receptor blocker/antagonist; GRF: glomerular filtration rate; hsCRP: high-sensitivity C-reactive protein

Table 2. Comparison of greyscale IVUS, NIRS and OCT data.

	Non-TCFA (n=58)	TCFA (n=18)	*p*-value
Greyscale IVUS analysis			
Reference:			
EEM CSA, mm^2 (IQR)	12.6 (11.1-16.4)	11.9 (10.2-15.6)	0.413
Lumen CSA, mm^2 (IQR)	7.2 (6.5-9.0)	7.3 (5.9-10.2)	0.765
Plaque and media CSA, mm^2 (IQR)	5.8 (3.6-7.5)	4.7 (3.2-6.8)	0.231
Plaque burden (%), SD	42±12	39±11	0.464
Minimum lumen site:			
EEM CSA, mm^2 (IQR)	12.7 (11.0-16.7)	14.6 (13.1-17.0)	0.043
Lumen CSA, mm^2 (IQR)	3.0 (2.1-4.8)	2.5 (1.5-3.4)	0.046
Plaque and media CSA, mm^2 (IQR)	9.6 (7.6-11.5)	12.3 (10.5-15.6)	0.001
Plaque burden (%), SD	72±14	80±9	0.005
Plaque volume, mm^3/cm (IQR)	67 (52-78)	92 (71-144)	0.001
Vessel volume, mm^3/cm (IQR)	112 (97-137)	124 (106-155)	0.164
Plaque length, mm (IQR)	10 (8-13)	21 (14-24)	<0.001
% Plaque volume, (IQR)	57 (50-64)	73 (65-124)	<0.001
Remodelling index, (IQR)	0.98 (0.88-1.07)	1.24 (1.11-1.26)	<0.001
Optical coherence tomography analysis			
Reference lumen CSA, mm^2 (IQR)	7.9 (6.7-9.7)	7.8 (5.2-9.2)	0.280
Minimal lesion lumen CSA, mm^2 (IQR)	2.5 (1.5-3.6)	1.6 (1.2-2.5)	0.025
Minimal cap thickness, µm (IQR)	111 (90-150)	50 (40-60)	<0.001
Maximal lipid arc °, (IQR)	164 (129-223)	313 (254-340)	<0.001
Plaque calcification	40 (69)	8 (44)	0.060
Plaque rupture, n (%)	0	10 (56)	<0.001
Thrombus, n	0	0	
Macrophages, n (%)	7 (16)	7 (41)	0.035
Near-infrared spectroscopy			
$LCBI_{2\ mm}$, (IQR)	200 (57-308)	538 (420-730)	<0.001
$LCBI_{4\ mm}$, (IQR)	176 (40-296)	480 (381-715)	<0.001
$LCBI_{8\ mm}$, (IQR)	128 (26-253)	415 (287-594)	<0.001
No lipid deposition, n (%)	10 (17)	0	0.059

CSA: cross-sectional area; EEM: external elastic membrane; IVUS : greyscale ultrasound; LCBI: lipid core burden index; QCA: quantitative coronary arteriography

operating characteristic (ROC) analysis was performed for independent NIRS and IVUS predictors of OCT-defined TCFA. The following optimal values for the detection of OCT-defined TCFA were determined in all coronary segments: 315 for $LCBI_{2\ mm}$, 265 for both $LCBI_{4\ mm}$ and $LCBI_{8\ mm}$, and 1.046 for RI **(Figure 3)**. The accuracy of IVUS and LCBI criterion values for OCT-defined TCFA detection were then assessed. Sensitivities, specificity, positive and negative predictive values for separate and combined IVUS and LCBI criterion values are presented in **Table 4**. **Figure 3** depicts the accuracy for OCT-defined TCFA detection by LCBI and RI criterion values. We observed the highest accuracy sensitivity and specificity values for $LCBI_{2\ mm}$ >315 with RI >1.046 as a single combined criterion value, with a sensitivity of 100% and a specificity of 91%. The sensitivity and utility of OCT (cap thickness <65 µm), NIRS ($LCBI_{2\ mm}$) and IVUS (RI) criteria for predicting TCFA and additional potential vulnerable lesions are presented in **Figure 4**.

INTER-OBSERVER VARIABILITY

The intraclass correlation coefficients for key parameters evaluated in this study were: reference OCT lumen CSA=0.871 (95% CI: 0.703-0.946); maximal lipid arc=0.904 (95% CI: 0.716-0.969); minimal cap thickness=0.909 (95% CI: 0.729-0.971). The kappa for inter-rater agreement for OCT-defined TCFA identification was 0.837 (95% CI: 0.700-0.974).

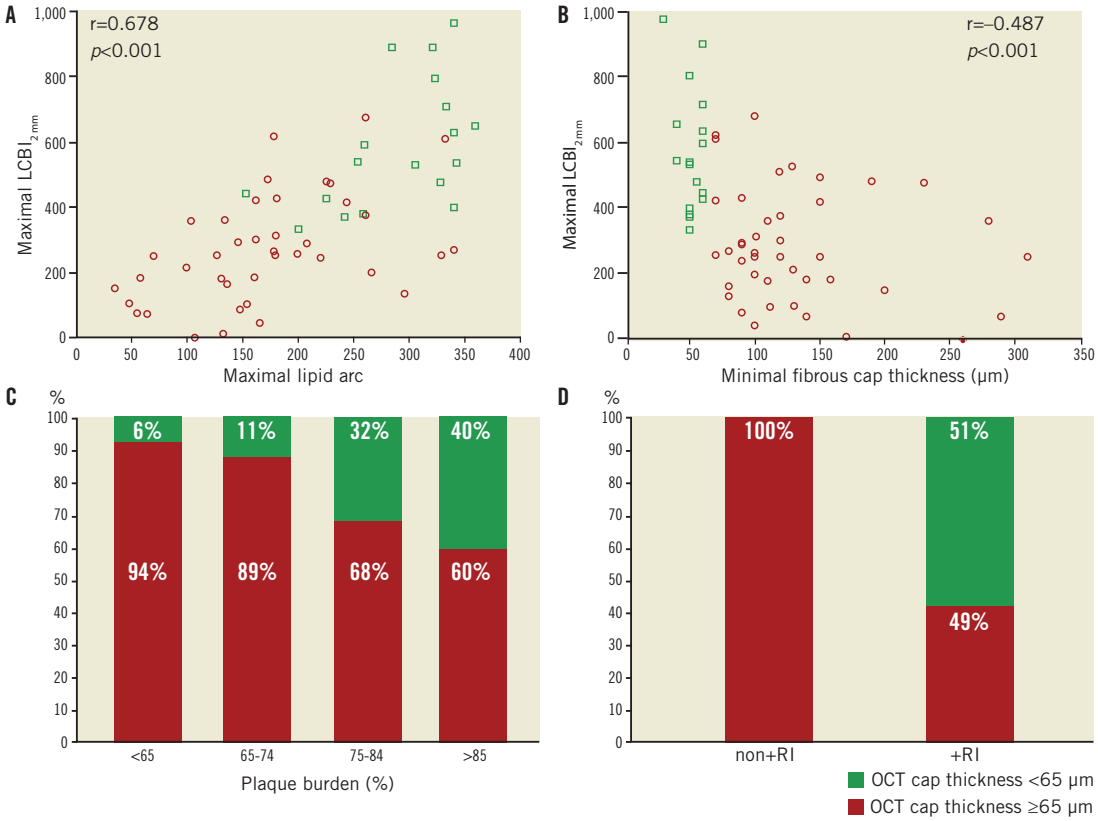

Figure 2. *NIRS and IVUS parameters vs. OCT-defined plaque characteristics. A) Correlation between maximal $LCBI_{2\,mm}$ vs. OCT-defined maximal lipid arc. B) Correlation between maximal $LCBI_{2\,mm}$ vs. OCT minimal cap thickness. C) Prevalence of OCT-defined TCFA vs. IVUS-determined plaque burden. D) Prevalence of OCT-defined TCFA vs. IVUS remodelling index (+RI: positive vessel remodelling; non+RI: not positively remodelled).*

Discussion

NIRS and greyscale IVUS have previously been used to assess plaque composition in acute coronary settings. These systems are available as a single analysis tool. NIRS has revealed that lesions responsible for acute coronary syndromes are lipid-rich compared to stable coronary lesions[18]. Greyscale IVUS studies have reported that lesions responsible for future acute coronary events exhibit a higher plaque burden and are associated with positive vessel

Table 3. Univariable and multivariable predictors of OCT-defined TCFA by binary logistic regression analysis of greyscale IVUS and NIRS parameters.

Predictors of OCT-defined thin-cap fibroatheroma							
Variable	Univariable analysis			Multivariable analysis			
	Odds ratio	95% CI	*p*-value	Wald chi-square	Odds ratio	95% CI	*p*-value
$LCBI_{2\,mm}$ (per 100 unit change)	2.8	1.7-4.7	<0.001	5.6	2.0	1.2-3.5	0.016
RI (per 0.1 unit change)	2.1	1.4-3.2	<0.001	4.6	2.0	1.1-3.7	0.031
Lesion length	1.3	1.1-1.4	<0.001	0.1	0.9	0.8-1.1	0.100
Plaque burden[a]	1.1	1.0-1.1	0.016	1.1	0.8	0.6-1.2	0.950
% Plaque volume[a]	1.1	1.0-1.2	0.007	Did not enter the model			
Minimal IVUS CSA	0.6	0.4-1.0	0.059	Did not enter the model			
$LCBI_{4\,mm}$ (per 100 unit change)	2.7	1.7-4.5	<0.001	Online Table 2[b]			
$LCBI_{8\,mm}$ (per 100 unit change)	3.1	1.8-5.5	<0.001	Online Table 3[b]			

[a]Plaque burden and % plaque volume are interdependent. Therefore, only plaque burden was entered into the multivariable model, because it is simpler to estimate by greyscale IVUS. [b]The multivariable logistic regression for $LCBI_{4\,mm}$ and $LCBI_{8\,mm}$ are presented in Online Tables 2 and 3, because further analysis revealed that $LCBI_{2\,mm}$ plus RI (as a single criterion) was superior for OCT-defined TCFA detection (Table 4). CSA: cross-sectional area; IVUS: greyscale ultrasound; LCBI: lipid core burden index; RI: remodelling index

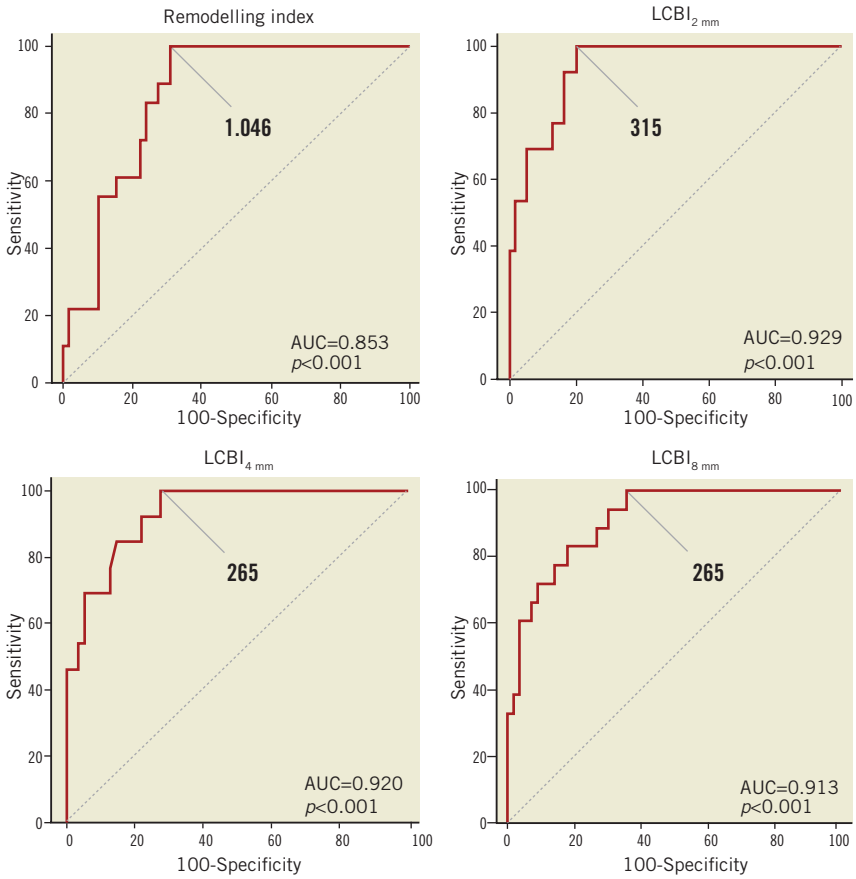

Figure 3. *Receiver operating characteristic (ROC) curves of RI and $LCBI_{2\ mm}$, $LCBI_{4\ mm}$, $LCBI_{8\ mm}$ for classifying OCT-defined TCFA. Values represent estimated cut-off values for RI and $LCBI_{2\ mm}$, $LCBI_{4\ mm}$, $LCBI_{8\ mm}$. AUC: area under the curve.*

remodelling[19-21]. The key finding of our study is that lipid-rich positively remodelled lesions, as assessed by dual NIRS-IVUS imaging, are likely to be thin-cap fibroatheromas.

Our results are of importance for a number of reasons. Firstly, our data extend those from greyscale IVUS[6], radiofrequency ultrasound (RF-IVUS)[22], integrated backscatter (IB-IVUS)[23] and computed tomography imaging[24], by demonstrating that positive vessel remodelling, high plaque burden and high lipid burden are associated with OCT-defined TCFA. Our findings are also in accord with a reported association of yellowish colour of the plaque detected by angioscopy with OCT-defined TCFA[25,26]. Furthermore, the presented prevalence of OCT-defined TCFA is consistent with the previous finding that plaque vulnerability is associated with the severity of angiographic vessel stenosis, plaque burden and positive vessel remodelling[4]. Moreover, the observed fibrous cap thickness in our study was similar to that observed in a prior OCT-based study in stable coronary patients[27]. Second, we documented that an increase in lipid core burden assessed by NIRS correlates with decreased minimal fibrous cap thickness assessed by OCT. This LCBI - minimal cap thickness correlation, together with higher LCBI values for OCT-defined TCFA, are in accord with RF-IVUS observations[22] and may explain a previous clinical observation regarding target coronary lesions. Madder at al reported generally higher LCBI values in coronary lesions responsible for acute coronary syndromes and lower LCBI values in plaques not responsible for acute syndromes. However, half of the lesions responsible for stable coronary syndromes were also lipid-rich[18]. In addition, prospective

Table 4. Diagnostic threshold of NIRS and greyscale IVUS to detect OCT-defined TCFA.

	Accuracy for OCT-defined TCFA detection			
	Sensitivity	Specificity	PPV	NPV
NIRS parameters				
$LCBI_{2\ mm}$ >315	100	77.6	58.1	100
$LCBI_{4\ mm}$ >265	100	74.1	54.5	100
$LCBI_{8\ mm}$ >265	83.3	82.1	60.0	93.9
IVUS parameters				
RI >1.046	100	68.9	50	100
NIRS and IVUS parameters				
$LCBI_{2\ mm}$ >315+RI >1.046	100	91	78	100
$LCBI_{4\ mm}$ >265+RI >1.046	100	88	72	100
$LCBI_{8\ mm}$ >265+RI >1.046	83	96	88	95

LCBI: lipid core burden index; NPV: negative predictive value; PPV: positive predictive value; RI: remodelling index

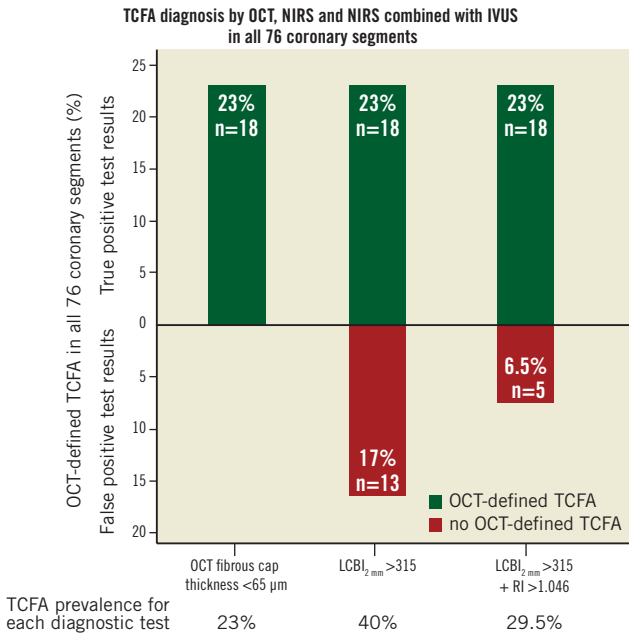

Figure 4. *Thin-cap atheroma and potential vulnerable plaque diagnosis for OCT, NIRS and combined NIRS and IVUS in 76 coronary segments. Sensitivity of OCT, NIRS and IVUS for diagnosis of potential vulnerable lesions is shown as number and percentage of lesions (from 76 total assessed lesions). Green columns (above x axis) represent OCT-defined TCFA with cap thickness <65 µm, while red columns (below x axis) represent potential vulnerable lesions that had OCT-defined cap thickness ≥65 µm but either $LCBI_{2\,mm}$ >315 alone or $LCBI_{2\,mm}$ >315 plus RI >1.046. Note that all lesions with cap thickness <65 µm (shown in green) also had $LCBI_{2\,mm}$ >315 and RI >1.046.*

studies have reported that identification of lipid-rich plaque increases the risk of future acute coronary syndromes[28,29]. Together with these reports, our data beget the important question as to whether some of these lipid-rich but stable plaques may ultimately evolve into TCFA. Third, our results confirmed that the maximal lipid arc assessed by OCT positively correlated with LCBI assessed by NIRS. This complements prior histological validations and demonstrates the validity of both systems for lipid detection and quantification[12]. Finally, we found that combined analysis of NIRS and greyscale IVUS parameters allows for accurate distinction between stable and vulnerable plaques. While single NIRS analysis was not sufficient for accurate OCT-defined TCFA detection, it was significantly improved by the additional greyscale IVUS analysis of the plaque. The greatest accuracy for OCT-defined TCFA detection was achieved using positive remodelling and $LCBI_{2\,mm}$ >315. Our findings are consistent with those of IB-IVUS and computed tomography angiography. Miyamoto et al established the utility of IB-IVUS accuracy for OCT-defined TCFA detection in plaques with high lipid core, positive remodelling and plaque burden >75%[23]. Computed tomography analysis showed that detection of lipid-rich plaque and lesions with RI >1.08 were independent predictors of OCT-defined TCFA[24].

Of interest, despite a vulnerable morphological pattern, a small number of lipid-rich and positively remodelled lesions exhibited a fibrous cap thickness of ≥65 µm by OCT. Hence, NIRS and IVUS might detect vulnerable plaques, but without severe thinning of the fibrous cap. Furthermore, prospective computed tomography studies have demonstrated that lipid-rich and positively remodelled lesions resulted in a greater likelihood of subsequent acute coronary syndrome during two years of follow-up[28]. Therefore, our data raise the provocative question as to whether the current definition of TCFA, being fibrous cap thickness <65 µm by OCT, adequately identifies all vulnerable lesions. However, we note that most ruptured TCFAs silently heal[30], and only 4.3% of TCFA were documented to be responsible for major adverse coronary events in three to four years of follow-up[29].

Several additional points are raised by our data. In contrast to previous autopsy studies, we did not observe thrombus formation at the site of plaque rupture. However, the study group consisted of stable patients heparinised before imaging, which might dissolve overlying thrombus before OCT imaging. In addition, although controversy has arisen regarding the prevalence of the calcium deposition in TCFAs, our findings are consistent with previous autopsy data[31].

Our data are of importance to clinical patient care. Firstly, these findings may help to stratify patients regarding the risk of future acute coronary syndromes and identify vulnerable plaques in the absence of OCT analysis. Thus NIRS-IVUS may also facilitate the assessment of ostial coronary lesions not amenable to OCT analysis, which may be a major advantage of NIRS-IVUS over OCT in terms of vulnerable plaque identification. In addition, by identifying stable lesions (low LCBI and absence of positive remodelling), dual NIRS-IVUS imaging may be used to identify when an invasive treatment might potentially be postponed in favour of medical treatment with aggressive lipid-lowering therapy and other agents. Germane to this possibility, aggressive lipid-lowering therapy has been reported to increase fibrous components of the plaque and decrease plaque vulnerability and lipid content[32,33].

Study limitations

The study group consisted of a relatively low number of patients and our findings require validation using a larger sample size. Although OCT is the gold standard for fibrous cap measurement *in vivo*, it is unclear if this is the optimal definition of a vulnerable plaque[34]. In addition, NIRS tissue penetration is limited and only provides information about the lipid content at a maximal depth of 1-2 mm into the vessel wall. Hence, NIRS is not informative about the proportion of lipid content in the deeper segments and essentially only provides information about the arc and longitudinal extent of lipid in the coronary vessel[12].

Conclusions

OCT-defined TCFA are characterised by positive vessel remodelling, a high plaque burden and greater lipid core burden as assessed

by dual NIRS-IVUS imaging. An explicit characterisation of plaque composition might help identify lesions which are responsive to extensive lipid reduction therapy and postpone interventional treatment without adversely affecting clinical outcomes.

Impact on daily practice

Our findings may help to identify vulnerable plaques by combined NIRS-IVUS imaging. It may be a new approach to assess the vulnerability of ostial coronary lesions not reachable for OCT analysis. This is a real advantage of NIRS-IVUS over OCT in terms of vulnerable plaque identification. Moreover, our results show that NIRS-IVUS provides a comprehensive assessment of coronary lesions that estimates their chemical composition, plaque burden and vessel remodelling, and identifies atheroma vulnerability.

Funding

All subjects in this study were also enrolled in the COLOR registry, which was supported by Infraredx, Inc. Infraredx also provided support for a clinical research imaging fellow who participated in this study. J. Kovacic is supported by National Institutes of Health Grant K08HL111330.

Conflict of interest statement

P. Moreno is a founder and a minor stockholder of Infraredx, Inc., the company that produces the near-infrared catheter used in this study. A. Kini acknowledges honoraria from Medscape and has received research grant support from Infraredx, Inc. S. K. Sharma acknowledges speaker's honoraria from Boston Scientific, Abbott Vascular, The Medicines Company and Lilly/DSI. The other authors have no conflicts of interest to declare.

References

1. Burke AP, Farb A, Malcom GT, Liang YH, Smialek J, Virmani R. Coronary risk factors and plaque morphology in men with coronary disease who died suddenly. *N Engl J Med.* 1997;336:1276-82.

2. Pasterkamp G, Schoneveld AH, van der Wal AC, Haudenschild CC, Clarijs RJ, Becker AE, Hillen B, Borst C. Relation of arterial geometry to luminal narrowing and histologic markers for plaque vulnerability: the remodeling paradox. *J Am Coll Cardiol.* 1998;32:655-62.

3. Varnava AM, Mills PG, Davies MJ. Relationship between coronary artery remodeling and plaque vulnerability. *Circulation*. 2002;105:939-43.

4. Yun KH, Mintz GS, Farhat N, Marso SP, Taglieri N, Verheye S, Foster MC, Margolis MP, Templin B, Xu K, Dressler O, Mehran R, Stone GW, Maehara A. Relation between angiographic lesion severity, vulnerable plaque morphology and future adverse cardiac events (from the Providing Regional Observations to Study Predictors of Events in the Coronary Tree study). *Am J Cardiol.* 2012;110:471-7.

5. Yabushita H, Bouma BE, Houser SL, Aretz HT, Jang IK, Schlendorf KH, Kauffman CR, Shishkov M, Kang DH, Halpern EF, Tearney GJ. Characterization of human atherosclerosis by optical coherence tomography. *Circulation*. 2002;106:1640-5.

6. Rathore S, Terashima M, Matsuo H, Kinoshita Y, Kimura M, Tsuchikane E, Nasu K, Ehara M, Asakura Y, Katoh O, Suzuki T. Association of coronary plaque composition and arterial remodelling: a optical coherence tomography study. *Atherosclerosis.* 2012;221:405-15.

7. Brezinski ME, Tearney GJ, Bouma BE, Boppart SA, Hee MR, Swanson EA, Southern JF, Fujimoto JG. Imaging of coronary artery microstructure (in vitro) with optical coherence tomography. *Am J Cardiol.* 1996;77:92-3.

8. Jang IK, Bouma BE, Kang DH, Park SJ, Park SW, Seung KB, Choi KB, Shishkov M, Schlendorf K, Pomerantsev E, Houser SL, Aretz HT, Tearney GJ. Visualization of coronary atherosclerotic plaques in patients using optical coherence tomography: comparison with intravascular ultrasound. *J Am Coll Cardiol.* 2002;39:604-9.

9. Yock PG, Linker DT. Intravascular ultrasound. Looking below the surface of vascular disease. *Circulation*. 1990;81:1715-8.

10. Nair A, Kuban BD, Tuzcu EM, Schoenhagen P, Nissen SE, Vince DG. Coronary plaque classification with intravascular ultrasound radiofrequency data analysis. *Circulation*. 2002;106:2200-6.

11. Pu J, Mintz GS, Brilakis ES, Banerjee S, Abdel-Karim AR, Maini B, Biro S, Lee JB, Stone GW, Weisz G, Maehara A. In vivo characterization of coronary plaques: novel findings from comparing greyscale and virtual histology intravascular ultrasound and near-infrared spectroscopy. *Eur Heart J.* 2012;33:372-83.

12. Gardner CM, Tan H, Hull EL, Lisauskas JB, Sum ST, Meese TM, Jiang C, Madden SP, Caplan JD, Burke AP, Virmani R, Goldstein J, Muller JE. Detection of lipid core coronary plaques in autopsy specimens with a novel catheter-based near-infrared spectroscopy system. *JACC Cardiovasc Imaging.* 2008;1:638-48.

13. Waxman S, Dixon SR, L'Allier P, Moses JW, Petersen JL, Cutlip D, Tardif JC, Nesto RW, Muller JE, Hendricks MJ, Sum ST, Gardner CM, Goldstein JA, Stone GW, Krucoff MW. In vivo validation of a catheter-based near-infrared spectroscopy system for detection of lipid core coronary plaques: initial results of the SPECTACL study. *JACC Cardiovasc Imaging.* 2009;2:858-68.

14. Moreno PR, Lodder RA, Purushothaman KR, Charash WE, O'Connor WN, Muller JE. Detection of lipid pool, thin fibrous cap, and inflammatory cells in human aortic atherosclerotic plaques by near-infrared spectroscopy. *Circulation*. 2002;105:923-7.

15. Kovacic JC, Lee P, Karajgikar R, Baber U, Narechania B, Suleman J, Moreno PR, Sharma SK, Kini AS. Safety of temporary and permanent suspension of antiplatelet therapy after drug eluting stent implantation in contemporary "real-world" practice. *J Interv Cardiol.* 2012;25:482-92.

16. Kovacic JC, Mehran R, Karajgikar R, Baber U, Suleman J, Kim MC, Krishnan P, Dangas G, Sharma SK, Kini A. Female gender and mortality after percutaneous coronary intervention: results from a large registry. *Catheter Cardiovasc Interv.* 2012;80:514-21.

17. Tahara S, Morooka T, Wang Z, Bezerra HG, Rollins AM, Simon DI, Costa MA. Intravascular optical coherence tomography detection of atherosclerosis and inflammation in murine aorta. *Arterioscler Thromb Vasc Biol.* 2012;32:1150-7.

18. Madder RD, Smith JL, Dixon SR, Goldstein JA. Composition of target lesions by near-infrared spectroscopy in patients with acute coronary syndrome versus stable angina. *Circ Cardiovasc Interv.* 2012;5:55-61.

19. Yamagishi M, Terashima M, Awano K, Kijima M, Nakatani S, Daikoku S, Ito K, Yasumura Y, Miyatake K. Morphology of vulnerable coronary plaque: insights from follow-up of patients examined by intravascular ultrasound before an acute coronary syndrome. *J Am Coll Cardiol.* 2000;35:106-11.

20. Schoenhagen P, Ziada KM, Kapadia SR, Crowe TD, Nissen SE, Tuzcu EM. Extent and direction of arterial remodeling in stable versus unstable coronary syndromes: an intravascular ultrasound study. *Circulation*. 2000;101:598-603.

21. Nakamura M, Nishikawa H, Mukai S, Setsuda M, Nakajima K, Tamada H, Suzuki H, Ohnishi T, Kakuta Y, Nakano T, Yeung AC. Impact of coronary artery remodeling on clinical presentation of coronary artery disease: an intravascular ultrasound study. *J Am Coll Cardiol.* 2001;37:63-9.

22. Sawada T, Shite J, Garcia-Garcia HM, Shinke T, Watanabe S, Otake H, Matsumoto D, Tanino Y, Ogasawara D, Kawamori H, Kato H, Miyoshi N, Yokoyama M, Serruys PW, Hirata K. Feasibility of combined use of intravascular ultrasound radiofrequency data analysis and optical coherence tomography for detecting thin-cap fibroatheroma. *Eur Heart J.* 2008;29:1136-46.

23. Miyamoto Y, Okura H, Kume T, Kawamoto T, Neishi Y, Hayashida A, Yamada R, Imai K, Saito K, Yoshida K. Plaque characteristics of thin-cap fibroatheroma evaluated by OCT and IVUS. *JACC Cardiovasc Imaging.* 2011;4:638-46.

24. Ito T, Terashima M, Kaneda H, Nasu K, Matsuo H, Ehara M, Kinoshita Y, Kimura M, Tanaka N, Habara M, Katoh O, Suzuki T. Comparison of in vivo assessment of vulnerable plaque by 64-slice multislice computed tomography versus optical coherence tomography. *Am J Cardiol.* 2011;107:1270-7.

25. Takano M, Jang IK, Inami S, Yamamoto M, Murakami D, Okamatsu K, Seimiya K, Ohba T, Mizuno K. In vivo comparison of optical coherence tomography and angioscopy for the evaluation of coronary plaque characteristics. *Am J Cardiol.* 2008;101:471-6.

26. Kubo T, Imanishi T, Takarada S, Kuroi A, Ueno S, Yamano T, Tanimoto T, Matsuo Y, Masho T, Kitabata H, Tanaka A, Nakamura N, Mizukoshi M, Tomobuchi Y, Akasaka T. Implication of plaque color classification for assessing plaque vulnerability: a coronary angioscopy and optical coherence tomography investigation. *JACC Cardiovasc Interv.* 2008;1:74-80.

27. Jang IK, Tearney GJ, MacNeill B, Takano M, Moselewski F, Iftima N, Shishkov M, Houser S, Aretz HT, Halpern EF, Bouma BE. In vivo characterization of coronary atherosclerotic plaque by use of optical coherence tomography. *Circulation*. 2005;111:1551-5.

28. Motoyama S, Sarai M, Harigaya H, Anno H, Inoue K, Hara T, Naruse H, Ishii J, Hishida H, Wong ND, Virmani R, Kondo T, Ozaki Y, Narula J. Computed tomographic angiography characteristics of atherosclerotic plaques subsequently resulting in acute coronary syndrome. *J Am Coll Cardiol.* 2009;54:49-57.

29. Stone GW, Maehara A, Lansky AJ, de Bruyne B, Cristea E, Mintz GS, Mehran R, McPherson J, Farhat N, Marso SP, Parise H, Templin B, White R, Zhang Z, Serruys PW; PROSPECT Investigators. A prospective natural-history study of coronary atherosclerosis. *N Engl J Med.* 2011;364:226-35.

30. Burke AP, Kolodgie FD, Farb A, Weber DK, Malcom GT, Smialek J, Virmani R. Healed plaque ruptures and sudden coronary death: evidence that subclinical rupture has a role in plaque progression. *Circulation*. 2001;103:934-40.

31. Burke AP, Taylor A, Farb A, Malcom GT, Virmani R. Coronary calcification: insights from sudden coronary death victims. *Z Kardiol.* 2000;89:49-53.

32. Hattori K, Ozaki Y, Ismail TF, Okumura M, Naruse H, Kan S, Ishikawa M, Kawai T, Ohta M, Kawai H, Hashimoto T, Takagi Y, Ishii J, Serruys PW, Narula J. Impact of statin therapy on plaque characteristics as assessed by serial OCT, grayscale and integrated backscatter-IVUS. *JACC Cardiovasc Imaging.* 2012;5:169-77.

33. Kini AS, Moreno P, Kovacic J, Limaye A, Ali Z, Sweeny J, Baber U, Dangas G, Sharma S. Does aggressive statin therapy reduce coronary atherosclerotic plaque lipid content? Results from: Reduction in Yellow Plaque by Aggressive Lipid Lowering Therapy (YELLOW) trial. *J Am Coll Cardiol.* 2012;59:E304-E304.

34. van Soest G, Regar E, Goderie TP, Gonzalo N, Koljenovic S, van Leenders GJ, Serruys PW, van der Steen AF. Pitfalls in plaque characterization by OCT: image artifacts in native coronary arteries. *JACC Cardiovasc Imaging.* 2011;4:810-3.

Online data supplement

Appendix. OCT and NIRS-IVUS image acquisition and analysis, statistical analysis.

Online Table 1. Comparison of angiographic data.

Online Table 2. Multivariable predictors of OCT-defined TCFA by binary logistic regression analysis of greyscale IVUS and NIRS LCBI values in 4 mm compartments.

Online Table 3. Multivariable predictors of OCT-defined TCFA by binary logistic regression analysis of greyscale IVUS parameters and NIRS LCBI values in 8 mm compartments.

Online data supplement

Appendix. OCT and NIRS-IVUS image acquisition and analysis, statistical analysis

OPTICAL COHERENCE TOMOGRAPHY IMAGE ACQUISITION

The commercially available C7-XR™ OCT Intravascular Imaging System (OCT C7 Dragonfly™; St. Jude Medical, St. Paul, MN, USA) was used for OCT image acquisition. The tip of the 2.7 Fr OCT catheter was placed at least 15 mm distally to the imaging target lesion. OCT image acquisition was then performed with continuous intracoronary contrast injection (Visipaque™; GE Healthcare Ltd, Little Chalfont, Buckinghamshire, UK), total volume 12-16 ml injected at 3-4 ml/sec, and simultaneous OCT catheter pullback at 20 mm/s. Each OCT catheter pullback imaged a total of 54 mm of the vessel.

OPTICAL COHERENCE TOMOGRAPHY IMAGE ANALYSIS

OCT image analysis scrutinised serial cross-sectional images of the vessel, at 1 mm intervals, using the LightLab Imaging Offline Review Station (LightLab Imaging, Inc./St. Jude Medical, Westford, MA, USA). Plaque composition was analysed as follows: signal-rich homogenous plaques were classified as fibrous, signal-poor regions with diffuse borders were classified as lipid, and signal-poor regions with well-defined borders were classified as calcified plaques. Additionally, macrophages were identified as bright spots[17]. The magnitude of lipid content was measured as the circumferential extent of lipid in OCT cross-sectional images and expressed in degrees (OCT lipid arc). Fibrous cap thickness was derived by measuring the thinnest signal-rich zone separating the lipid content from the vessel lumen (μm). The thinnest part of the fibrous cap was measured three times and its average was defined as the fibrous cap thickness. OCT-defined TCFA was defined as a lipid-rich plaque with fibrous cap thickness <65 μm. In addition, the presence of both plaque rupture and/or luminal thrombus was noted during OCT analysis.

Cross-sectional area (CSA), and minimal and maximal diameter of the vessel were measured every 1 millimetre. The smallest CSA in one segment was taken as the OCT-defined minimal CSA. The OCT reference lumen area was estimated as the largest CSA within 10 mm proximally or distally to the minimal lumen CSA in the scanned coronary segment.

NEAR-INFRARED SPECTROSCOPY AND INTRAVASCULAR ULTRASOUND IMAGE ANALYSIS

COMBINED NIRS AND GREYSCALE IVUS IMAGE ACQUISITION

Combined NIRS and greyscale IVUS image acquisition was performed using the commercially available TVC Imaging System™ with the 2.4 Fr TVC Insight Catheter (Infraredx, Inc., Burlington, MA, USA). The tip of the TVC catheter was positioned at least 10 mm distal to the imaging target lesion. Subsequently, the automated pullback was 0.5 mm/sec (240 rotations/min) until the TVC catheter entered the guiding catheter.

NIRS IMAGE ANALYSIS

The raw spectra of NIRS estimate the probability of the presence of an atherosclerotic lipid core and measurements are displayed as a chemogram – a digit code map. The chemogram is transformed into a colour-coded, red to yellow scaled NIRS map (7-bit), which represents a spectroscopic image of the scanned vessel. The NIRS map's X-axis indicates the combined NIRS-IVUS pullback position in millimetres, and the Y-axis indicates its circumferential position in degrees. Each pixel on the NIRS map represents the probability of lipid core. Red pixels correspond to a low and yellow pixels to a high probability of lipid core. Pixels with insufficient data (e.g., caused by guidewire shadowing) appear as black.

The NIRS map analysis allows calculation of the lipid core burden index (LCBI). LCBI is estimated by dividing yellow pixels per all pixels (without black ones) within the analysed pullback compartment and are expressed per mill (‰). In the present study, the maximal LCBI was estimated in 2 mm, 4 mm and 8 mm pullback compartments for every analysed lesion ($LCBI_{2\ mm}$, $LCBI_{4\ mm}$, $LCBI_{8\ mm}$). NIRS map analysis was performed using Lipiscan LS107.001rB software (Infraredx).

GREYSCALE INTRAVASCULAR ULTRASOUND IMAGE ANALYSIS

Quantitative greyscale IVUS measurements were performed every one millimetre in scanned coronary segments using QIvus version 2.1 (Medis, Leiden, The Netherlands). Cross-sectional images were quantified for lumen CSA, external elastic lamina (EEM) CSA, plaque and media CSA and plaque burden. Plaque and media CSA were calculated as the difference between EEM CSA and lumen CSA. Plaque burden was calculated as plaque and media CSA divided by EEM CSA x 100 (%) at the minimal CSA site.

The IVUS reference lumen area was estimated as the largest CSA within 10 mm located proximally or distally to the minimal lumen CSA in one analysed coronary segment. The reference EEM CSA was calculated as an average of the proximal and distal EEM CSA with the smallest plaque burden, but not higher than 50%. If either the proximally or distally evaluated plaque burden was ≥50%, then the proximal or distal EEM CSA with the least plaque burden served as the reference.

A lesion was defined as the region between the proximal and distal EEM reference sites or as the region between either the proximal or the distal EEM reference site and a side branch delimiting the assessed coronary segment. Remodelling index (RI) was calculated by dividing EEM CSA at the site of minimal lumen CSA by reference EEM CSA. Lesions with RI ≤0.95 were defined as negatively remodelled, while those with an RI ≥1.05 were defined as positively remodelled. An RI between these values was taken as a non-remodelled vessel.

In every lesion, a lumen vessel volume and EEM volume was calculated based on Simpson's rule (mm^3/cm). These data were used to estimate plaque volume (EEM volume - vessel volume, mm^3/cm) and % plaque volume (100 x [plaque volume] / EEM volume, %).

STATISTICAL ANALYSIS

The Kolmogorov-Smirnov test assessed the obtained data distribution. For normally distributed values data are presented as mean with standard deviation (SD), for non-normally distributed values data are presented as median with interquartile intervals (IQR, 25th percentile, 75th percentile). Normally distributed data were compared using Pearson's correlation and unpaired t-test, while non-normally distributed data were compared using Spearman's rank correlation and the Mann-Whitney test. The categorical data were compared using Fisher's exact test or chi-square test.

Univariable and multivariable logistic regression was performed to identify predictors of OCT-defined TCFA. The accuracy of estimated independent predictors for OCT-defined TCFA and the criterion values for NIRS and IVUS measurements were evaluated by receiver operating characteristic (ROC) curves.

The intraclass correlation coefficient and inter-rater agreement (kappa) were evaluated to assess inter-observer variability (MedCalc software version 12.2.1; MedCalc, Ostend, Belgium).

Online Table 1. Comparison of angiographic data.

	Non-TCFA (n=58)	TCFA (n=18)	*p*-value
Angiographic data			
Left anterior descending artery, n (%)	27 (47)	8 (44)	
Left circumflex artery, n (%)	8 (14)	5 (28)	
Right coronary artery, n (%)	23 (39)	5 (28)	0.348
Type of lesion:			
A/B1, n (%)	20 (35)	4 (22)	
B2/C, n (%)	38 (65)	14 (78)	0.334
Location of lesion:			
Proximal, n (%)	20 (35)	3 (17)	
Mid, n (%)	31 (53)	13 (72)	
Distal, n (%)	7 (12)	2 (11)	0.319
Quantitative coronary angiography data:			
Reference lumen diameter (mm), SD	3.2±0.7	3.1±0.5	0.636
Minimum lumen diameter, mm (IQR)	1.2 (0.9-1.6)	0.9 (0.7-1.2)	0.057
Diameter of stenosis (%), SD	60±19	75±11	0.002

Online Table 2. Multivariable predictors of OCT-defined TCFA by binary logistic regression analysis of greyscale IVUS and NIRS LCBI values in 4 mm compartments.

Predictors of OCT-defined thin-cap fibroatheroma				
Variable	Multivariable analysis			
	Wald chi-square	Odds ratio	95% CI	*p*-value
$LCBI_{4\,mm}$ [a]	5.9	2.0	1.1-3.6	0.014
RI [b]	5.1	2.1	1.1-3.9	0.021
Plaque length	2.8	1.1	0.9-1.3	0.089
Plaque burden	0.0	1.0	0.8-1.1	0.988
Minimal IVUS CSA	Did not enter the model			

[a] $LCBI_{4\,mm}$ values were divided by 100 to present odds ratio for every 100 increase in LCBI value. [b] RI values were multiplied by 10 to present odds ratio for every 0.1 increase in RI value.

Online Table 3. Multivariable predictors of OCT-defined TCFA by binary logistic regression analysis of greyscale IVUS parameters and NIRS LCBI values in 8 mm compartments.

Predictors of OCT-defined thin-cap fibroatheroma				
Variable	Multivariable analysis			
	Wald chi-square	Odds ratio	95% CI	*p*-value
$LCBI_{8\,mm}$ [a]	5.9	2.0	1.1-3.6	0.017
RI [b]	5.1	2.1	1.1-3.9	0.016
Plaque length	2.8	1.1	0.9-1.3	0.137
Plaque burden	0.0	1.0	0.8-1.1	0.967
Minimal IVUS CSA	Did not enter the model			

[a] $LCBI_{8\,mm}$ values were divided by 100 to present odds ratio for every 100 increase in LCBI value. [b] RI values were multiplied by 10 to present odds ratio for every 0.1 increase in RI value.